

INADVERT: An Interactive and Adaptive Counterdeception Platform for Attention Enhancement and Phishing Prevention

Linan Huang, *Student Member, IEEE*, and Quanyan Zhu, *Member, IEEE*

Abstract

Deceptive attacks exploiting the innate and the acquired vulnerabilities of human users have posed severe threats to information and infrastructure security. This work proposes INADVERT, a systematic solution that generates interactive visual aids in real-time to prevent users from inadvertence and counter visual-deception attacks. Based on the eye-tracking outcomes and proper data compression, the INADVERT platform automatically adapts the visual aids to the user's varying attention status captured by the gaze location and duration. We extract system-level metrics to evaluate the user's average attention level and characterize the magnitude and frequency of the user's mind-wandering behaviors. These metrics contribute to an adaptive enhancement of the user's attention through reinforcement learning. To determine the optimal hyper-parameters in the attention enhancement mechanism, we develop an algorithm based on Bayesian optimization to efficiently update the design of the INADVERT platform and maximize the accuracy of the users' phishing recognition.

Index Terms

Attention Enhancement, Phishing Attack Prevention, Gaze Tracking, Human Vulnerability in Cybersecurity, Reinforcement Learning, Bayesian Optimization.

I. INTRODUCTION

Human is often considered as the weakest link in cybersecurity. Adversaries can exploit human errors and vulnerabilities, such as social engineering and phishing, to launch deceptive attacks that would lead to information leakages and data breaches. Moreover, these attacks often serve as the initial stages of sophisticated attacks, including supply chain attacks and Advanced Persistent Threats (APTs), which inflict tremendous damage on critical infrastructures. We classify human vulnerabilities into innate vulnerabilities (e.g., bounded attention and rationality) and acquired vulnerabilities (e.g., lack of security awareness and incentive). The acquired vulnerabilities can be mitigated through security training, rule enforcement, and incentive designs [1], but these methods are insufficient to deal with the innate ones. In addition, the unpredictability and heterogeneity of human behaviors make it even harder to mitigate human vulnerabilities. To this end, there is a need for security-assistive technologies to deter and adaptively correct the user misbehavior resulted from the innate vulnerabilities.

In this work, we focus on inattention, one type of innate human vulnerabilities, and use phishing email as a case study to explore the users' visual behaviors when they determine whether a received email is secure or not. We design a computer interface that interacts with human participants in real-time to record their eye-tracking data and security decisions. Based

L. Huang and Q. Zhu are with the Department of Electrical and Computer Engineering, New York University, Brooklyn, NY, 11201, USA. E-mail:{lh2328,qz494}@nyu.edu

on the data, we develop INADVERT¹, a human-centric anti-deception platform, to efficiently generate optimal visual aids to guide and sustain the users' attention to the right content of the email. The design of the INADVERT platform contains two feedback loops at different time scales, as shown in Fig. 1.

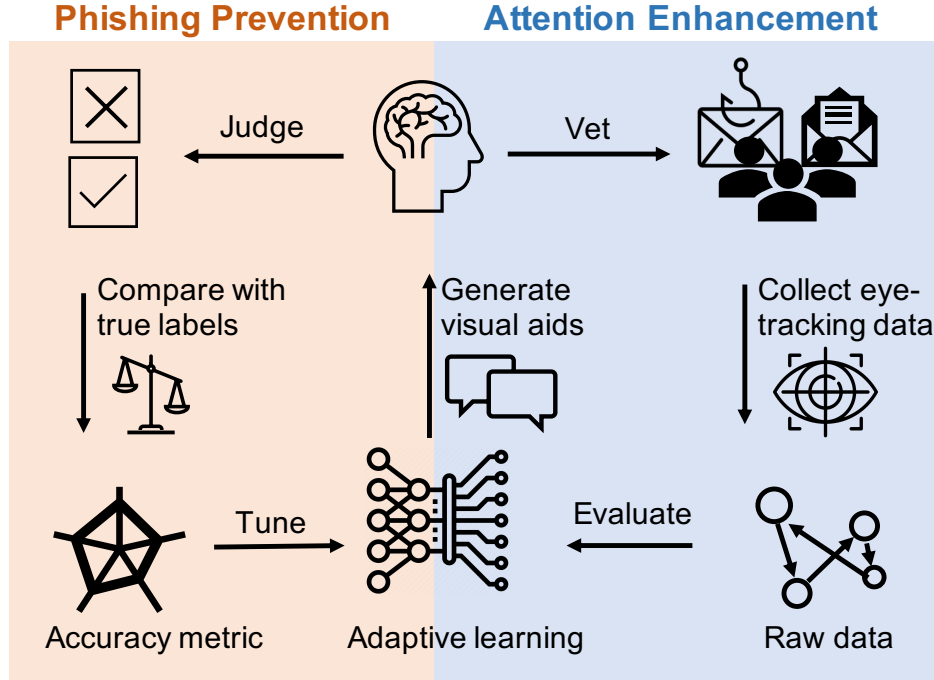


Fig. 1: The design diagram of INADVERT. The adaptive learning loops of the attention enhancement mechanism and the phishing prevention mechanism are highlighted using juxtaposed blue and orange backgrounds, respectively.

The blue background in the right part of Fig. 1 illustrates how we design an interactive human-machine interface and visual aids (e.g., highlighting, warnings, and educational messages) to engage participants in email processing. Human participants are presented with a sequence of emails and asked to classify them as phishing or normal while wearing eye trackers. As they vet the emails, the eye tracker records their eye gaze data which manifests their hidden cognitive states. We evaluate the raw data in real-time to monitor each user's average attention level assigned to the Areas of Interest (AoIs) of the emails. In contrast to low-level eye-tracking metrics related to fixations, saccades, regressions, and backtracks in the previous works [2], [3], we propose system-level security metrics to evaluate the magnitude and the frequency of the user's mind-wandering behaviors. Based on the security metrics and the evaluation results, we generate the visual aids from a predefined visual-aid library to direct the participant's attention to the desired AoIs. The visual aids change the user's hidden cognitive states and lead to the set of eye-tracking data with different patterns of attention level and mind-wandering, which then updates the design of visual aids. Thus, the optimal design of the visual aids is learned iteratively during the experiment.

The orange background in the left part of Fig. 1 illustrates how we tune the interface configuration and the attention evaluation parameters to safeguard users from phishing emails. While

¹INADVERT is an acronym for INteractive Anti-Deception Visual aids for Efficient Real-time security-assistive Technology.

reading the emails, the participants are also asked to identify whether they are phishing or normal. Then, we compare their judgments with the true labels of the emails to evaluate the accuracy of their security decisions. Leveraging Bayesian optimization theory, we propose an efficient tuning algorithm to improve their accuracy. Since the participants need to focus and sustain attention for a while to make a security decision, the tuning feedback loop denoted in orange updates less frequently than the feedback loop of attention enhancement denoted in blue.

The INADVERT provides an interactive and adaptive solution to counteract inattention and improve the human recognition of phishing attacks. The data-driven approach achieves customized solutions in terms of the users and the content of the emails. The feedback learning framework enables an automatic and systematic design of the optimal visual support system. Our preliminary results corroborate the efficiency of INADVERT; i.e., it adapts to the optimal interaction configuration within 6 iterations. As a corrective measure, INADVERT applies to other security threats caused by inattention and contributes to a systematic and quantitative solution for compensating innate human vulnerabilities. We may also embed INADVERT into VR/AR technologies to mitigate human vulnerabilities under simulated deception scenarios, where the simulated environment can be easily repeated or changed.

II. RELATED WORKS

A. Phishing attack detection and prevention

Phishing is the act of masquerading as a legitimate entity to serve malware or steal credentials. The authors in [4] have identified the following three human vulnerabilities that make humans the unwitting victims of phishing.

- Lack of computer system knowledge or the knowledge of security and security indicators; e.g., www.ebay-members-security.com does not belong to www.ebay.com.
- Inadequacy to identify visual deception; e.g., the phishing email can contain an image of a legitimate hyperlink, but the image itself serves as a hyperlink to a malicious site [4]. A human cannot judge whether a hyperlink is an image by merely looking at it.
- Lack of attention (e.g., careless users fail to notice the phishing indicators such as spelling errors and grammar mistakes) and *inattentional blindness* (e.g., users focusing on reading the main content fail to perceive unloaded logos in a phishing email [5]).

Many works have attempted to mitigate the above three human vulnerabilities to prevent phishing attacks. First, user security education and anti-phishing training, e.g., role-playing phishing simulation games [6] and fake phishing attacks [7], have been used to compensate for the user's lack of security knowledge and increase users' security awareness. Second, detection techniques based on visual similarities [8] and machine learning [9] have been applied to help users identify visual deception. Third, passive warnings (the warning does not block the content-area) and active warnings (the warning prohibits the user from viewing the content-data) have been adopted to draw users' attention and prevent them from falling victim to phishing [9], [10].

B. Counterdeception technologies

Adversarial cyber deception has been a long-standing problem. It is easy for an attacker to deceive yet much more difficult for regular users to identify the deception given the universal human vulnerabilities. Previous works have mainly focused on technical solutions, e.g., defensive deception technologies [11]–[13], to deter, detect, and respond to deceptive attacks. This work focuses on designing human-centric solutions to counteract adversarial cyber deception.

Biosensors such as eye trackers and electroencephalogram (EEG) devices provide a window into an analytical understanding of human perception and cognition to enhance security and privacy [14]. In particular, researches have investigated the users' gaze behaviors and attention when reading Uniform Resource Locators (URLs) [3], phishing webs [15], and phishing email [16]–[18]. These works illustrate the users' visual processing of phishing contents [3], [15], [17], [19] and the effects of visual aids [18]. The authors in [15] further establish correlations between eye movements and phishing identification to estimate the likelihood that users may fall victim to phishing attacks. Compared to these works that *analyze* human perception, we use eye-tracking data to *modify* the processes of human perception and decisions. Moreover, we define proper metrics to measure the user's attention level and the accuracy of phishing identification, enabling the optimal design of the visual support system to counteract visual deception and phishing.

III. INTERFACE DESIGN AND GAZE PLOT

We conducted a user study on a group of human participants who vet a list of emails and classify them as phishing or normal while wearing the Tobii Pro eye tracker. Fig. 2 illustrates the tentative human-machine interface that consists of a control panel, an email display area, and a distraction area. The human participants can click the back and the next buttons on the top to go forward and backward between emails. Then, they make their security decisions by clicking the thumb up or the thumb down icons. The participants do not need to make decisions in the given sequence of the email list; i.e., they have the freedom to assign their time and attention before the decision-making. However, once they have clicked the thumb icon, the decision cannot be changed, and the email with a decision is removed from the email list. To simulate the daily works and entertainments that occupy the human user's scarce attention, we add a distraction area where a video or a movie is continuously played as a visual distraction.

We use Tobii Pro Glasses 3 to record the participants' gaze location (where they look) and the gaze duration (how long they look) in real-time. The sampling rate is 50 Hz, and the raw data from the eye tracker is noisy due to biological noise, e.g., the Ocular MicroTremor (OMT), ambient illumination, and sensor uncertainty. Signal processing tools can help us to obtain a noiseless gaze plot shown in Fig. 2. The number in each blue circle represents the participant's gaze location in time sequence, and its size is proportional to the gaze duration. It shows that the participant reads the email from top to bottom and spends more time on the main content than other areas. The gaze location changes consecutively for most of the time, but jumps and repeats can happen during the reading process.

We elaborate on the two feedback loops of Fig. 1 in Section IV and V, respectively. Throughout the paper, we use subscript to index the time and the stage. Calligraphic letter \mathcal{S} defines a set and $|\mathcal{S}|$ represents its cardinality. The indicator function $\mathbf{1}_{\{A\}}$ takes value 1 if condition A is true and value 0 if A is false.

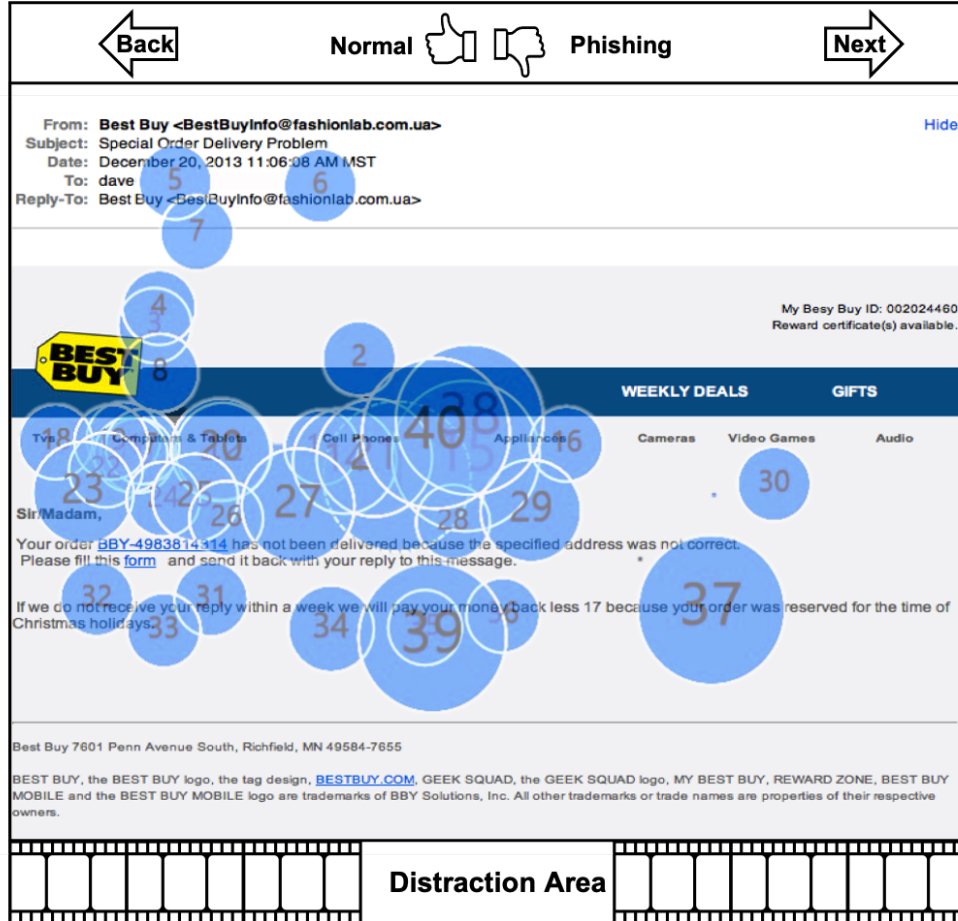


Fig. 2: The human-machine interface consists of a control panel on the top, an email display area in the middle, and a distraction area at the bottom. The blue circles illustrate an exemplary gaze plot.

IV. ATTENTION ENHANCEMENT MECHANISM

The gaze plot in Fig. 2 tracks the changes in the participants' visual behaviors. However, the comprehensive sensory outcomes can take up a significant amount of space to store, and it can be challenging to process and evaluate the outcomes in real-time. Therefore, we need to compress the sensory outcomes and remove the information that hardly contributes to attention evaluation and phishing recognition. Previous works [3], [15], [17] have identified the role of Areas of Interest (AoIs) in helping human users recognize phishing. Thus, we aggregate the potential gaze locations (i.e., pixels of the email area) into a finite number of I AoIs that include the email address, the subject line, the addressee, attachments, hyperlinks, and the phishing indicators such as misspellings and grammar mistakes. We index these non-overlapping AoIs by $i \in \mathcal{I} := \{1, 2, \dots, I\}$. Each email does not need to contain all the AoIs and the AoIs are invisible to the participants. We refer to all other areas in the emails (e.g., blank areas) as the *uninformative area*.

A. Visual state transition model

Based on the AoI to which the participant's gaze location belongs at different times, we establish a state-transition model for a total of T seconds. We define $\mathcal{S} := \{s^i\}_{i \in \mathcal{I}} \cup \{s^{ua}, s^{da}\}$ as the set of $I+2$ *visual states*, where s^i represents the i -th AoI, s^{ua} represents the uninformative area, and s^{da} represents the distraction area. We provide an example transition map of these visual states in Fig. 3. The links represent the potential shifts of the gaze locations during the

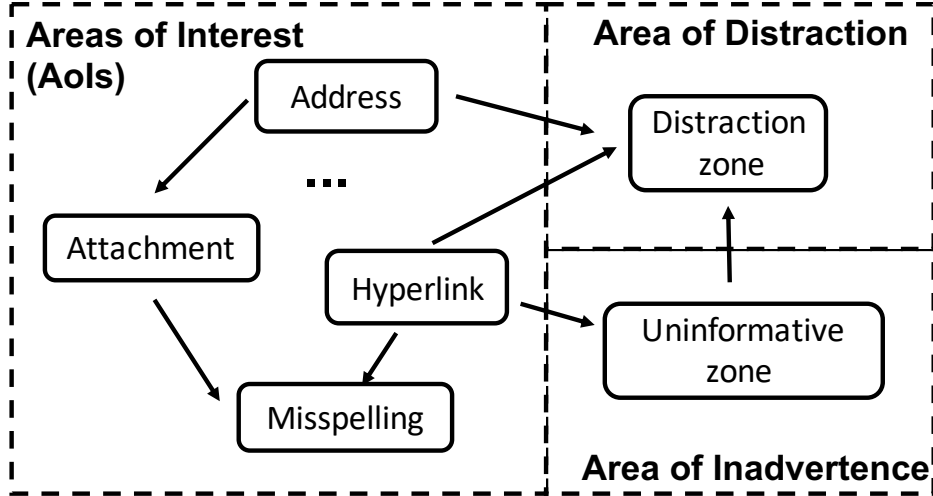


Fig. 3: Transitions among visual states in \mathcal{S} .

experiment; e.g., the participants can shift their focus from the email address to the attachment or the distraction area. We omit most links for illustration purposes; e.g., it is also possible for a participant to regain attention to the AoIs from distraction or inadvertence.

We denote the participant's visual state at time $t \in [0, T]$ as $s_t \in \mathcal{S}$. Then, each participant's *gaze path* during the interval $[0, T]$ can be characterized as a stochastic process $[s_t]_{t \in [0, T]}$. The stochastic transition of the visual states divides the entire time interval $[0, T]$ into different *transition stages*. We visualize an exemplary gaze path $[s_t]_{t \in [0, T]}$ in Fig. 4 under $I = 4$ AoIs and $T = 50$ seconds. As denoted by the colored squares, 40 visual states arrive in sequence, which results in 40 discrete transition stages. Compared to the gaze plot in Fig. 2 that records the gaze locations across the entire email area, the gaze path in Fig. 4 aggregates these gaze locations into merely 6 visual states, enabling the real-time attention evaluation and phishing recognition.

In this work, we do not distinguish among the human participants concerning their attention processes; i.e., we assume that $[s_t]_{t \in [0, T]}$ from each human participant belongs to the same class of stochastic processes. After collecting the eye-tracking data from W human participants sequentially or simultaneously, we cascade the W sets of data into one that lasts for WT seconds. Thus, without loss of generality, we can consider $W = 1$ human participant.

B. Visual support system

One feature that distinguishes our work from the previous works is that our human-machine interface provides a visual support system to properly guide and sustain the participants' attention on the AoIs of the email, which consequently enhances their abilities to recognize phishing. To achieve the goal, we first establish a library of possible visual aids. For example, we can consider

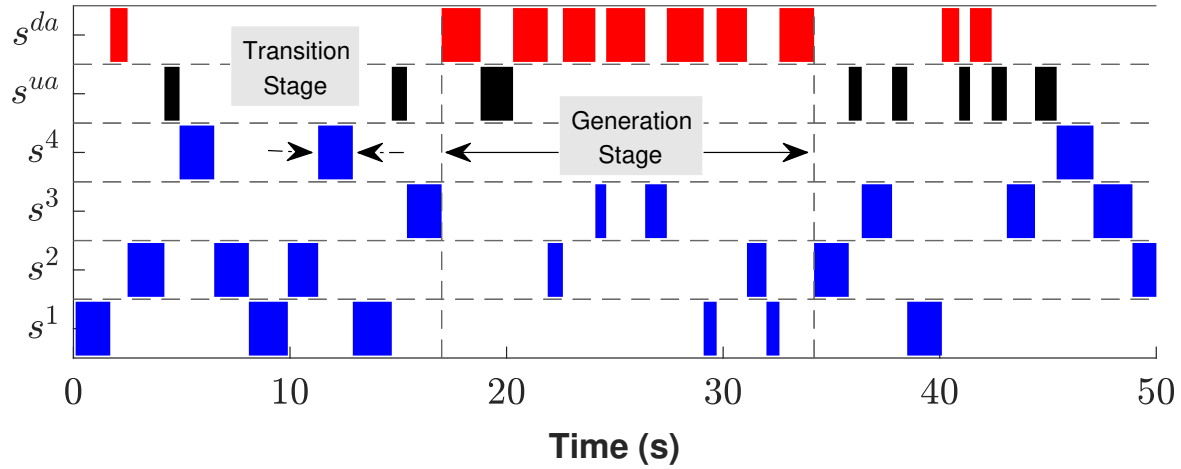


Fig. 4: An exemplary gaze path $[s_t]_{t \in [0, T]}$. The x -axis and the y -axis represent $T = 50$ seconds and $I + 2 = 6$ visual states, respectively. We denote visual states s^{da} , s^{ua} , and $\{s^i\}_{i \in \mathcal{I}}$, in red, black, and blue, respectively. Each generation stage contains different numbers of transition stages.

three classes of visual aids, i.e., a highlight of AoIs to attract attention, a passive or active warning to prevent the participant from clicking suspicious hyperlinks and attachments, and a sequence of educational messages that show the participant several phishing examples. We define the visual-aid library as a finite set \mathcal{A} and each possible design of visual aid is denoted by $a \in \mathcal{A}$.

The visual aid is generated with a period of length T^{pl} and we refer to the time interval between every two visual aids as the *generation stage* indexed by $k \in \mathcal{K} := \{1, 2, \dots, K\}$, where K is the maximum generation stage during $[0, T]$; i.e., $KT^{pl} \leq T$ and $(K+1)T^{pl} \geq T$. Then, we denote $a_k \in \mathcal{A}$ as the visual aid at the k -th generation stage. Fig. 4 illustrates how visual aids affect the transition of visual states in $K = 3$ generation stages divided by the two vertical dashed lines. During the second generation stage, the visual support system generates an improper visual aid, which leads to more frequent transitions to the distraction area and also a longer sojourn time at the visual state s^{da} . On the contrary, the proper visual aids during the first and the third generation stages engage the users and extend their attention span, i.e., the amount of time spent on AoIs before a transition to s^{da} or s^{ua} .

C. Attention evaluation and visual-aid design

Different visual aids can affect the participant's visual behaviors in a beneficial (e.g., timely highlights prevent users from mind-wandering) or detrimental way (e.g., extensive highlights make participants weary and less attentive to the AoIs). Due to the unpredictability and heterogeneity of human behaviors and their mental processes, no off-the-shelf theory or design rules can generate the most beneficial visual aids. Thus, we apply model-free reinforcement learning in Section IV-C4 to iteratively find the optimal design of visual aids from the pre-defined library \mathcal{A} . To this end, we assign scores to each visual state in Section IV-C1 to evaluate the participant's attention (i.e., gaze at AoIs) and inattention (i.e., gaze at uninformative and distraction areas). The scores can be determined manually based on the expert recommendation and empirical studies, e.g., [19], or adaptively based on the feedback-learning approach in Section V. Then,

we extract representative metrics to evaluate the participant's average attention level and the mind-wandering behaviors in Section IV-C2 and IV-C3, respectively.

Our metric-based method further reduces the space to storage and the time to process the gaze-path data in Fig. 4, enabling the adaptive visual-aid design in real-time. Moreover, it preserves the participants' privacy as the gaze path can reveal sensitive information about their biometric identity, gender, age, and ethnicity [20], [21].

1) *Transient and concentration rewards*.: Both the gaze location and the gaze duration matter in the identification of phishing attacks. For example, at the first glance, users cannot distinguish the spoofed email address 'paypa1@mail.paypaI.com' from the authentic one 'paypal@mail.paypal.com' while a close look reveals that the lower case letter 'l' is replaced by the number '1' and the capital letter 'I'. Therefore, we assign the *transient reward* $r^{tr}(s^i) \in \mathbb{R}^+$ and the *concentration reward* $r^{co}(s^i, \tau) \in \mathbb{R}^+$ to encourage the users' transient attention and the sustained attention of duration τ , respectively, to the i -th AoI.

These rewards can be different for each AoI. For example, paying attention to the phishing indicators is assigned a low concentration reward, since transient attention is sufficient to identify the misspellings and grammar mistakes. On the contrary, paying attention to AoIs, such as the address and the hyperlinks, is assigned a high concentration reward, since a longer attention span extracts more information, e.g., the substitution of letter l into I, to identify the phishing email. Analogously, the negative scores $r^{tr}(s^i) \in \mathbb{R}^-$ and $r^{co}(s^i, \tau) \in \mathbb{R}^-$ penalize the participant's transient and sustained attention, respectively, to the undesired visual states $s^i, i \in \{ua, da\}$.

2) *Average attention level*.: Based on the sets of scores associated with $s \in \mathcal{S}$, we define the cumulative reward $u_k(s, t)$ at time $t \in [(k-1)T^{pl}, kT^{pl}]$ over generation stage $k \in \mathcal{K}$ as

$$u_k(s, t) := r^{tr}(s) \cdot \mathbf{1}_{\{\exists \tau \in [(k-1)T^{pl}, t] \text{ s.t. } s_\tau = s\}} + g_k^{co}(r^{co}, s, t).$$

If the gaze path at the interval $[(k-1)T^{pl}, t]$ includes visual state $s \in \mathcal{S}$ at some time τ , i.e., $s_\tau = s$, then we add the transient reward $r^{tr}(s)$ as shown in the first term. In the second term, the cumulative concentration reward g_k^{co} is defined to be a monotone function of $t \in [(k-1)T^{pl}, kT^{pl}]$, e.g.,

$$g_k^{co}(r^{co}, s, t) := \int_{(k-1)T^{pl}}^t r^{co}(s, \tau - (k-1)T^{pl}) \cdot e^{-\alpha(\tau - (k-1)T^{pl})} \cdot \mathbf{1}_{\{s_\tau = s\}} d\tau.$$

Since the amount of information that a user can extract from an AoI is limited, we use $\alpha \in \mathbb{R}^+$ to penalize the rate of concentration reward as time elapses.

Averaging over all visual states, $v_k(t) := \sum_{s \in \mathcal{S}} u_k(s, t)$ represents the participant's *average attention level* over time interval $[(k-1)T^{pl}, t]$. Since $v_k(t)$ is bounded for all $k \in \mathcal{K}, t \in [(k-1)T^{pl}, kT^{pl}]$, we can quantize its value into M values that form a finite set denoted by \mathcal{X} . We represent the quantized value of $v_k(t) \in \mathbb{R}$ as $v_k^{qu}(t) \in \mathcal{X}$ for all $k \in \mathcal{K}, t \in [(k-1)T^{pl}, kT^{pl}]$ and define the quantized average attention level over each generation stage in Definition 1.

Definition 1 (Quantized average attention level). We define $\bar{v}_k := v_k(kT^{pl})$ and $\bar{v}_k^{qu} := v_k^{qu}(kT^{pl})$ as the participant's average attention level and quantized average attention level over generation stage $k \in \mathcal{K}$, respectively.

We visualize $v_k(t)$ in Fig. 5 based on the exemplary gaze path in Fig. 4. There are $K = 3$ generation stages during which the value of $v_k(t)$ increases and decreases with time t when $s_t \in \{s^i\}_{i \in \mathcal{S}}$ and $s_t \in \{s^{ua}, s^{da}\}$, respectively.

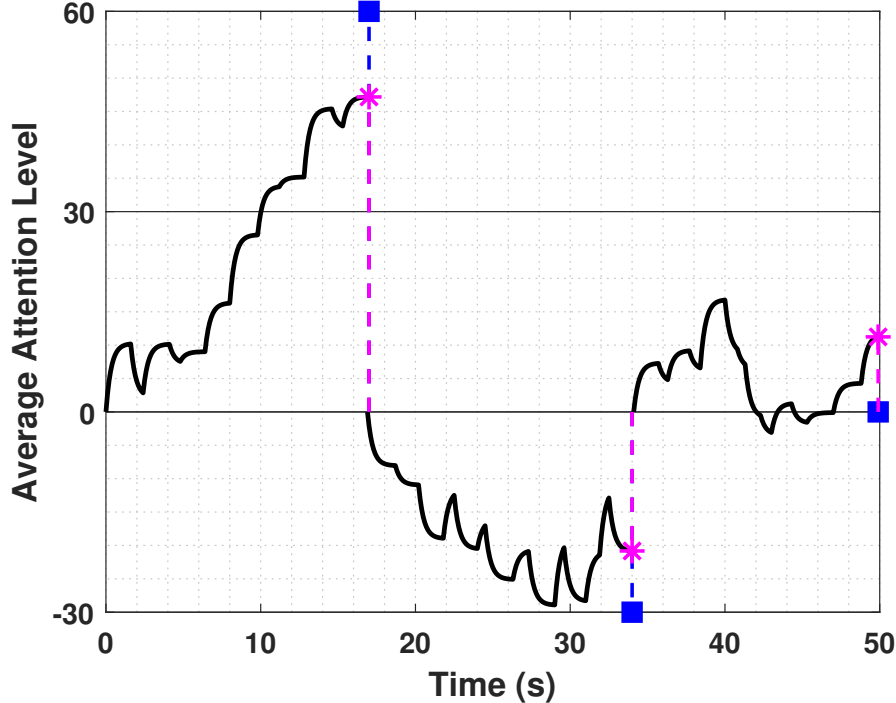


Fig. 5: The participant's average attention level $v_k(t), k \in \mathcal{K}, t \in [(k-1)T^{pl}, kT^{pl}]$, over $K = 3$ generation stages in $T = 50$ seconds. The horizontal lines quantize $v_k(t)$ into $M = 4$ values that form the finite set $\mathcal{X} = \{-30, 0, 30, 60\}$. The purple star and the blue square denote \bar{v}_k and \bar{v}_k^{qu} , respectively.

3) *Other system-level metrics.*: Besides the (quantized) average attention level, we propose other system-level metrics, defined in Definition 2, 3, and 4, from $v_k(t)$ to capture different features of attention.

Definition 2 (Range of attention fluctuation). We define the peak-to-peak amplitude $\bar{v}_k^{ar} := \max_{t \in [(k-1)T^{pl}, kT^{pl}]} v_k(t) - \min_{t \in [(k-1)T^{pl}, kT^{pl}]} v_k(t)$ as the range of attention fluctuation during the generation stage $k \in \mathcal{K}$.

Definition 3 (Magnitude of mind-wandering). At time $t \in [(k-1)T^{pl}, kT^{pl}]$, the user is said to be mind-wandering of magnitude $(\varepsilon^{up}, \varepsilon^{do})$ if $v_k(t) > \max\{v_k(t - \tau_0) + \varepsilon^{up}, v_k(t + \tau_0) + \varepsilon^{do}\}$, where $\tau_0 > 0$ is a pre-defined parameter.

To measure the frequency of mind-wandering over the continuous-time interval $[(k-1)T^{pl}, kT^{pl}]$, we discretize the interval into a finite number of stages. Then, we can count the total number of mind-wandering of magnitude $(\varepsilon^{up}, \varepsilon^{do})$ at these discrete stages and denote the number as $n_k(\varepsilon^{up}, \varepsilon^{do})$.

Definition 4 (Frequency of mind-wandering). Given the magnitude level $(\varepsilon^{up}, \varepsilon^{do})$, the user is said to be $n_k(\varepsilon^{up}, \varepsilon^{do})$ -frequent mind-wandering during the generation stage $k \in \mathcal{K}$.

In each generation stage $k \in \mathcal{K}$, the magnitude level $(\varepsilon^{up}, \varepsilon^{do})$ affects the frequency $n_k(\varepsilon^{up}, \varepsilon^{do})$ as shown in Fig. 6 with $\varepsilon^{up} = 0$ and $\varepsilon^{do} \in [0, 4]$. Based on the definition, $n_k(\varepsilon^{up}, \varepsilon^{do})$ decreases

as the values of ϵ^{up} and ϵ^{do} increase for any $k \in \mathcal{K}$.

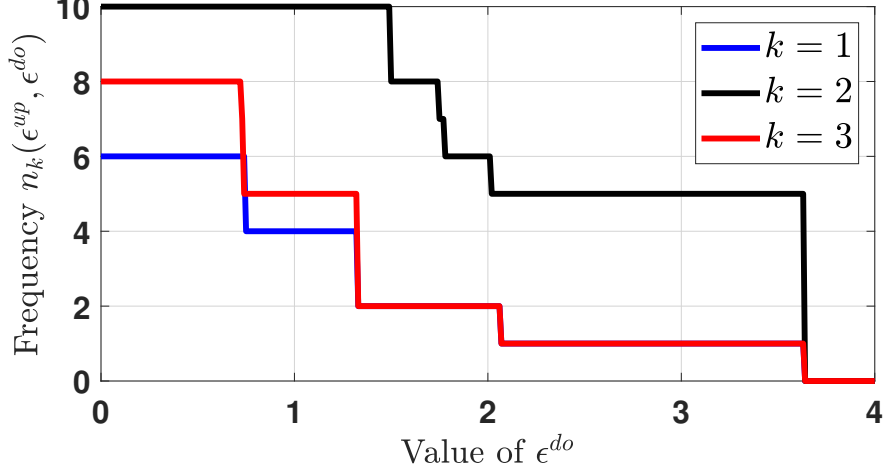


Fig. 6: Frequency of mind-wandering in $K = 3$ generation stages represented by the blue, black, and red lines, respectively.

For most values of ϵ^{do} (i.e., $\epsilon^{do} \in [1.3, 3.6]$), Fig. 6 distinguishes $n_2(\epsilon^{up}, \epsilon^{do})$ in black from $n_1(\epsilon^{up}, \epsilon^{do})$ in blue and $n_3(\epsilon^{up}, \epsilon^{do})$ in red. This distinction results from the fact that the visual aids during the second generation stage (resp. the first and the third generation stages) are improperly (resp. properly) designed, as illustrated in Section IV-B. Thus, the metric $n_k(\epsilon^{up}, \epsilon^{do})$ reflects the quality of the visual aids; i.e., a proper visual aid should engage users and thus lead to less frequency in mind-wandering of large magnitude.

Previous works, e.g., [17], [19], have defined attention metrics based on the AoIs, e.g., the proportion of time spent on each AOI, gaze duration means, fixation count, and average duration. Compared to these low-level metrics extracted directly from eye-gaze data, we propose system-level attention metrics based on the sufficient statistics, e.g., $v_k(t)$, of the eye-gaze data $[s_t]_{t \in [0, T]}$, which preserve the user privacy. Moreover, by assigning scores to each visual state, we manage to *quantify* the features (i.e., the magnitude and frequency) of the user's visual behaviors such as mind-wandering in email reading and phishing recognition.

4) *Adaptive visual-aid design via Q-learning*.: Since the visual aids are generated periodically at the end of each generation stage, we refer to the quantized average attention level $\bar{v}_k^{qu} \in \mathcal{X}$ as the *attention state* at the generation stage $k \in \mathcal{K}$. With the quantization error between $v_k(t)$ and $\bar{v}_k^{qu}(t)$, the value of the attention state is approximately proportional to the average attention level. Thus, we can assign a linear reward function $R(\bar{v}_k^{qu}) := \bar{v}_k^{qu}$ to each attention state $\bar{v}_k^{qu} \in \mathcal{X}$ and apply *Q*-learning to determine the optimal visual aid $a_k^* \in \mathcal{A}$ at each generation stage $k \in \mathcal{K}$.

The *Q*-table $[Q_k(\bar{v}_k^{qu}, a_k)]_{\bar{v}_k^{qu} \in \mathcal{X}, a_k \in \mathcal{A}}$ represents the *attention pattern* at generation stage $k \in \mathcal{K}$; i.e., the expected payoff of generating visual aid $a_k \in \mathcal{A}$ when the quantized average attention level is $\bar{v}_k^{qu} \in \mathcal{X}$. Let the learning rate γ_k satisfy $\sum_{k=0}^{\infty} \gamma_k = \infty$ and $\sum_{k=0}^{\infty} (\gamma_k)^2 < \infty$. With a given discounted factor $\beta \in (0, 1)$, we can update the attention pattern at each generation stage $k \in \mathcal{K}$ as follows, i.e.,

$$Q_{k+1}(\bar{v}_k^{qu}, a_k^*) = (1 - \gamma_k)Q_k(\bar{v}_k^{qu}, a_k^*) + \gamma_k[R(\bar{v}_k^{qu}) + \beta \max_{a \in \mathcal{A}} Q_k(\bar{v}_{k+1}^{qu}, a)],$$

where the optimal visual aid a_k^* is implemented and updated iteratively at each generation stage $k \in \mathcal{K}$ as follows, i.e., $a_k^* = \arg \max_{a \in \mathcal{A}} Q_k(\bar{v}_k^{qu}, a)$. The user's privacy is preserved because

our learning method uses the visual aids as the feedback of the high-level attention states at generation stages rather than the low-level visual states at transition stages.

V. PHISHING PREVENTION MECHANISM

The attention enhancement mechanism in Section IV engages participants in vetting emails and serves as a stepping-stone to achieving the ultimate goal of phishing prevention. However, empirical evidences and observations such as the Yerkes–Dodson law [22] have shown that a high attention level, or mental arousal, does not necessarily yield good performance. Thus, besides those attention metrics, e.g., the average attention level, we need to design accuracy metrics to measure the users' performance of phishing recognition as shown in Section V-A.

In Section V-B, we develop an efficient algorithm to tune the hyper-parameters in the attention enhancement mechanism, i.e., the interface configuration (the period length T^{pl} to generate visual aids) and the attention evaluation parameters (the transient reward r^{tr} and the concentration reward r^{co}). Letting $r^{co}(s, \tau) = \bar{r}^{co}(s)$ be independent of the time duration τ , we denote these hyper-parameters as one d -dimensional variable $\theta := [r^{tr}(s)_{s \in \mathcal{S}}, \bar{r}^{co}(s)_{s \in \mathcal{S}}, T^{pl}] \in \mathbb{R}^d$ where $d := 2|\mathcal{S}| + 1$. We assume that the i -th element θ^i is upper and lower bounded by $\bar{\theta}^i$ and $\underline{\theta}^i$, respectively. Thus, $\theta \in \Theta^d := \{[\theta^i]_{i \in \{1, \dots, d\}} \in \mathbb{R}^d | \underline{\theta}^i \leq \theta^i \leq \bar{\theta}^i\}$. Finally, we evaluate the efficiency of the algorithm in Section V-C.

A. Accuracy of phishing recognition

We first provide the metric to evaluate the outcome of participants' phishing identification under a given hyper-parameter $\theta \in \Theta^d$. While vetting these emails, the participants are asked to judge whether the emails are phishing (denoted by z^{ph}) or normal (denoted by z^{no}) by clicking the thumb up or the thumb down icons in Fig. 2. The true label of the emails, either phishing (denoted by y^{ph}) or normal (denoted by y^{no}) are unknown to the participants throughout the experiment. We denote the participant's n -th judgment as $z_n^\theta \in \{y^{ph}, y^{no}\}$ and the true label of the email as $y_n^\theta \in \{y^{ph}, y^{no}\}$. Once the participant has judged N emails, we define the following *accuracy metric* $c^{ac}(\theta)$ to evaluate the accuracy of the phishing recognition, i.e.,

$$c^{ac}(\theta) := \sum_{n=1}^N (\mathbf{1}_{\{z_n^\theta = z^{ph}\}} - \mathbf{1}_{\{y_n^\theta = y^{no}\}})^2, \forall \theta \in \Theta^d.$$

We can also choose the following metrics to measure the accuracy.

- True positive rate

$$c^{tp}(\theta) := \frac{\sum_{n=1}^N \mathbf{1}_{\{z_n^\theta = z^{ph}, y_n^\theta = y^{ph}\}}}{\sum_{n=1}^N \mathbf{1}_{\{z_n^\theta = z^{ph}, y_n^\theta = y^{ph}\}} + \sum_{n=1}^N \mathbf{1}_{\{z_n^\theta = z^{no}, y_n^\theta = y^{ph}\}}}.$$

- Precision

$$c^{pr}(\theta) := \frac{\sum_{n=1}^N \mathbf{1}_{\{z_n^\theta = z^{ph}, y_n^\theta = y^{ph}\}}}{\sum_{n=1}^N \mathbf{1}_{\{z_n^\theta = z^{ph}, y_n^\theta = y^{ph}\}} + \sum_{n=1}^N \mathbf{1}_{\{z_n^\theta = z^{ph}, y_n^\theta = y^{no}\}}}.$$

- F-score

$$c^{fs}(\theta) := 2c^{tp}(\theta) / (1 + c^{tp}(\theta) / c^{pr}(\theta)).$$

Our goal is to find the optimal hyper-parameter $\theta^* \in \Theta^d$ to maximize the accuracy of phishing identification; i.e., $\theta^* = \arg \max_{\theta \in \Theta^d} c^{ac}(\theta)$. However, we cannot know the value of $c^{ac}(\theta)$ for

a $\theta \in \Theta^d$ a priori until we implement this hyper-parameter θ in the attention enhancement mechanism. The implemented hyper-parameter affects the visual aids which change the participant's average attention level and the performance of phishing identification measured by $c^{ac}(\theta)$. Since the experimental evaluation at a given $\theta \in \Theta^d$ is time-consuming, we present an algorithm in Section V-B to determine how to choose and update the hyper-parameter to maximize the detection accuracy.

B. Efficient hyper-parameter tuning

As illustrated in Fig. 7, we refer to the duration of every N security decisions as a *tuning stage*. Assume that the experiment and time budgets restrict us to conduct L tuning stages in total. We denote θ_l as the hyper-parameter at the l -th tuning stage where $l \in \mathcal{L} := \{1, 2, \dots, L\}$. Since the participants are not timed to make decisions, each tuning stage can contain different numbers of generation stages.

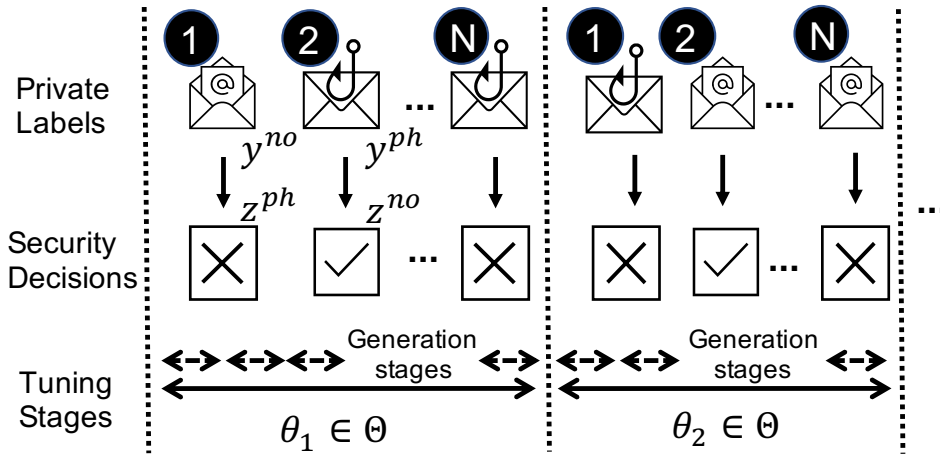


Fig. 7: Hyper-parameter tuning based on the participant's security decisions. Each tuning stage consists of N decisions and lasts for different numbers of generation stages.

To find the optimal hyper-parameter $\theta^* \in \Theta^d$ within L trials is challenging. The empirical methods such as a naive grid search and random search over $\Theta^d \subset \mathbb{R}^d$ become inefficient when $d > 1$. Bayesian Optimization (BO) methods [23] provide a systematic way to update the hyper-parameter and balance between exploration and exploitation. BO consists of a Bayesian statistical model of the objective function c^{ac} and an acquisition function for deciding the hyper-parameter to implement at the next tuning stage.

The statistical model of c^{ac} is a Gaussian process $\mathcal{N}(\mu^0, \Sigma^0)$ with the mean function $\mu^0(\theta) = \bar{\mu}^0$ and covariance function or kernel $\Sigma^0(\theta, \bar{\theta}) = \lambda^0 \cdot \exp(\sum_{i=1}^d \lambda^i (\theta^i - \bar{\theta}^i)^2)$ for all $\theta, \bar{\theta} \in \Theta^d$, where $\bar{\mu}^0$, λ^0 and $\lambda^i, i \in \{1, 2, \dots, d\}$, are parameters of the kernel. The kernel Σ^0 is required to be positive semi-definite and has the property that the points closer in the input space are more strongly correlated. For any $l \in \mathcal{L}$, we define three shorthand notations $\mu^0(\theta_{1:l}) := [\mu^0(\theta_1), \dots, \mu^0(\theta_l)]$, $c^{ac}(\theta_{1:l}) := [c^{ac}(\theta_1), \dots, c^{ac}(\theta_l)]$, and

$$\Sigma^0(\theta_{1:l}, \theta_{1:l}) := \begin{bmatrix} \Sigma^0(\theta_1, \theta_1) & \dots & \Sigma^0(\theta_1, \theta_l) \\ \vdots & \ddots & \vdots \\ \Sigma^0(\theta_l, \theta_1) & \dots & \Sigma^0(\theta_l, \theta_l) \end{bmatrix}.$$

Then, the evaluation vector of $l \in \mathcal{L}$ elements is assumed to be multivariate Gaussian distributed, i.e., $c^{ac}(\theta_{1:l}) \sim \mathcal{N}(\mu^0(\theta_{1:l}), \Sigma^0(\theta_{1:l}, \theta_{1:l}))$. Conditioned on the values of $\theta_{1:l}$, we can infer the value of $c^{ac}(\theta)$ at any other $\theta \in \Theta \setminus \{\theta_{l'}\}_{l' \in \{1, \dots, l\}}$ by Bayesian rule, i.e.,

$$c^{ac}(\theta) | c^{ac}(\theta_{1:l}) \sim \mathcal{N}(\mu^n(\theta), (\Sigma^n(\theta))^2), \quad (1)$$

where $\mu^n(\theta) = \Sigma^0(\theta, \theta_{1:l}) \cdot \Sigma^0(\theta_{1:l}, \theta_{1:l})^{-1} \cdot (c^{ac}(\theta_{1:l}) - \mu^0(\theta_{1:l})) + \mu^0(\theta)$ and $(\Sigma^n(\theta))^2 = \Sigma^0(\theta, \theta) - \Sigma^0(\theta, \theta_{1:l}) \cdot \Sigma^0(\theta_{1:l}, \theta_{1:l})^{-1} \cdot \Sigma^0(\theta_{1:l}, \theta)$.

We adopt *expected improvement* as the acquisition function. Define $c_l^* := \max_{l' \in \{1, \dots, l\}} c^{ac}(\theta_{l'})$ as the optimal evaluation among the first l evaluations and a shorthand notation $(c^{ac}(\theta) - c_l^*)^+ := \max\{c^{ac}(\theta) - c_l^*, 0\}$. For any $l \in \mathcal{L}$, we define $\mathbb{E}_l[\cdot] := \mathbb{E}[\cdot | c^{ac}(\theta_{1:l})]$ as the expectation taken under the posterior distribution of $c^{ac}(\theta)$ conditioned on the values of l evaluations $c^{ac}(\theta_{1:l})$. Then, the expected improvement is $\text{EI}_l(\theta) := \mathbb{E}_l[(c^{ac}(\theta) - c_l^*)^+]$. The hyper-parameter at the next tuning stage is chosen to maximize the expected improvement at the current stage, i.e.,

$$\theta_{l+1} = \arg \max_{\theta \in \Theta^d} \text{EI}_l(\theta). \quad (2)$$

The expected improvement can be evaluated in a closed form, and (2) can be computed inexpensively by gradient methods [23].

At the first $L^0 \in \{1, 2, \dots, L\}$ tuning stages, we choose the hyper-parameter $\theta_l, l \in \{1, 2, \dots, L^0\}$ uniformly from Θ^d . We can use the evaluation results $c^{ac}(\theta_l), l \in \{1, 2, \dots, L^0\}$, to determine the parameters $\bar{\mu}^0, \lambda^0$, and $\lambda^i, i \in \{1, 2, \dots, d\}$, by Maximum Likelihood Estimation (MLE); i.e., we determine the values of these parameters so that they maximize the likelihood of observing the vector $[c^{ac}(\theta_{1:L^0})]$. For the remaining $L - L^0$ tuning stages, we choose $\theta_l, l \in \{L^0, L^0 + 1, \dots, L\}$, in sequence as summarized in Algorithm 1.

Algorithm 1: Hyper-parameter tuning via BO.

- 1 **Implement** the initial L^0 evaluations $c^{ac}(\theta_l), l \in \{1, 2, \dots, L^0\}$;
- 2 **Place** a Gaussian process prior on c^{ac} , i.e., $c^{ac}(\theta_{1:L^0}) \sim \mathcal{N}(\mu^0(\theta_{1:L^0}), \Sigma^0(\theta_{1:L^0}, \theta_{1:L^0}))$;
- 3 **for** $l \leftarrow L^0$ **to** L **do**
- 4 **Obtain** the posterior distribution of $c^{ac}(\theta)$ in (1) based on the existing l evaluations;
- 5 **Compute** $\text{EI}_l(\theta), \forall \theta \in \Theta^d$, based on the posterior distribution;
- 6 **Determine** θ_{l+1} via (2);
- 7 **Implement** θ_{l+1} at the next tuning stage $l + 1$ to evaluate $c^{ac}(\theta_{l+1})$;
- 8 **end**
- 9 **Return** θ_L at the final tuning stage as the optimal hyper-parameter;

C. Algorithm evaluation

We evaluate the efficiency of Algorithm 1 for $d = 1$ and $L^0 = 1$, and illustrate $L = 6$ iterations in Fig. 8 where $\Theta^d = [1, 10]$. The unknown objective function c^{ac} is assumed to be the black line, which has two local optima. At the first tuning stage $l = 1$ in Fig. 8a, we randomly choose the hyper-parameter $\theta_1 \in \Theta^d$ denoted by the red dot. Then, we update the statistic model, i.e., the Gaussian distribution denoted by the error bar plot in blue, and the acquisition function EI_1 denoted by the red line. Based on the Gaussian process model and the kernel Σ^0 , two hyper-parameters closer to each other are more strongly correlated. Thus, the error bar plot assigns more

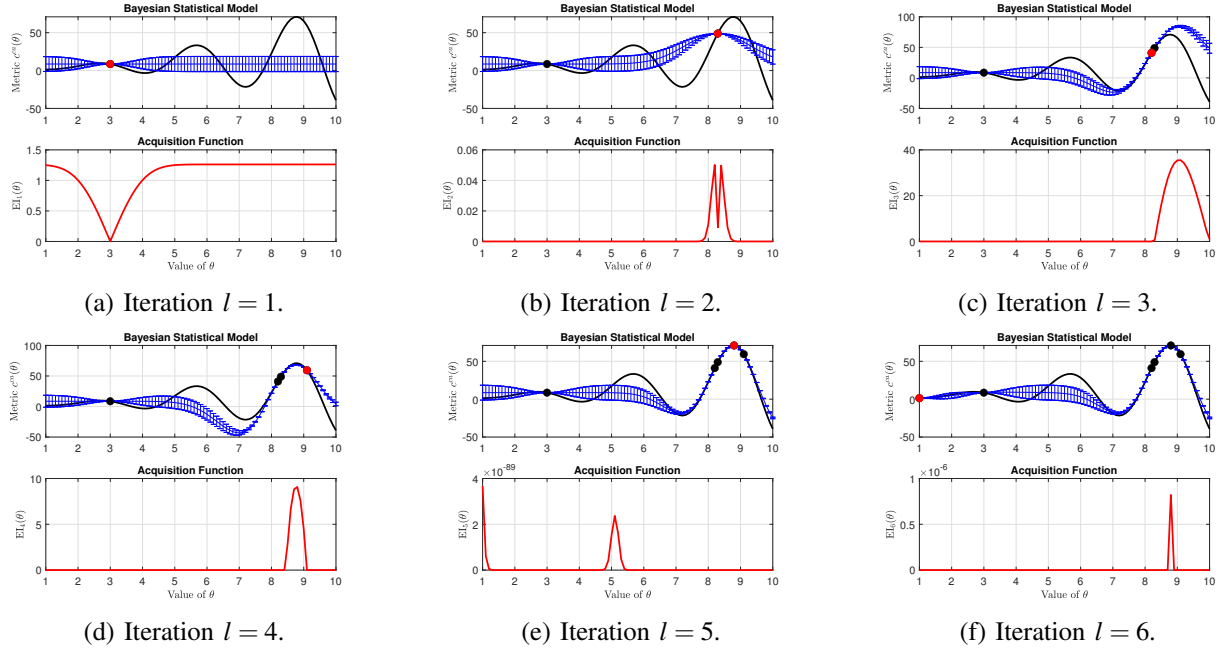


Fig. 8: Hyper-parameter selection for $L = 6$ tuning stages. The black line represents the objective function c^{ac} , and the error bar plot in blue represents the Gaussian process model of c^{ac} . The red line and the red dot represent the expected improvement function EI_l and the implemented hyper-parameter θ_l , respectively. The black dots represent the previously implemented hyper-parameters $\theta_{1:l-1}$.

uncertainty (denoted by a larger error bar) for the hyper-parameters far from the implemented one.

We maximize the acquisition function to obtain $\theta_2 \in \Theta^d$ to implement at the second tuning stage $l = 2$. Since the maximizer of EI_1 is not unique, we break the tie randomly and implement θ_2 denoted by the red dot in Fig. 8b. Then, we update the statistic model and the acquisition function at the second tuning stage. Analogously, we obtain the remaining figures in Fig. 8. The acquisition function in red strikes a balance between exploration (i.e., implementing the hyper-parameters that lead to high uncertainty, e.g., see Fig. 8a, 8b, and 8f) and exploitation (i.e., implementing the hyper-parameters that lead to a high value of $c^{ac}(\theta)$, e.g., see Fig. 8c, 8d, and 8e).

The results show that the algorithm manages to escape the two local optima and select the optimal hyper-parameter $\theta^* = \arg \max_{\theta \in \Theta^d} c^{ac}(\theta)$ within 6 iterations. Moreover, the Gaussian statistic model achieves an accurate estimate of the true objective function $c^{ac}(\theta)$, especially in the region $\theta \in [7, 10]$ near the global optimal θ^* .

VI. CONCLUSIONS AND FUTURE WORK

Lack of attention is one of the main reasons why users fall victim to phishing attacks. In this work, we have developed an interactive and adaptive counterdeception platform called INADVERT to guide the users' attention to the right contents of the email and consequently improve their accuracy in phishing recognition. To enable a real-time evaluation of the user's visual behaviors, we have built AoIs from the entire email area and a transition model of AoIs to

compress the comprehensive eye-tracking data into a representative stochastic gaze path. After assigning transient and concentration rewards to encourage transient and sustained attention, respectively, on the AoIs, we have defined privacy-preserving and light-weight metrics to evaluate the user's average attention level and the mind-wandering behaviors. Based on these attention metrics, we have used model-free reinforcement learning methods to adapt the visual-aid design to the user's attention status.

Using the attention enhancement mechanism as a stepping-stone, we have designed an efficient algorithm to increase the user's accuracy of phishing recognition by tuning the interface configuration and the attention evaluation parameters. The update of these hyper-parameters at each tuning stage revises the visual aids, affects the users' attention, and consequently improves the accuracy of phishing recognition. The preliminary results have shown that the algorithm strikes a balance of exploration and exploitation, and can efficiently update the INADVERT platform to the optimal interaction setting within 6 iterations.

Human plays significant roles in cybersecurity. It is challenging to model and quantify human behaviors and their mental processes such as cognition and attention. By adopting a data-driven approach and two learning feedback of different time scales, this work has laid out a theoretical foundation to *analyze*, *evaluate*, and finally *modify* the human attention process while humans make security decisions of phishing recognition. The future work would focus on designing a more sophisticated visual support system that can determine when and how to generate visual aids in lieu of a periodic generation. We would allow the participants to report their confidence levels while they make the security decisions. Finally, there would be an opportunity to incorporate factors such as pressure and incentives into the design by limiting the participant's vetting time and providing rewards for accurately identifying phishing, respectively.

REFERENCES

- [1] L. Huang and Q. Zhu, "Game of duplicity: A proactive automated defense mechanism by deception design," *arXiv preprint arXiv:2006.07942*, 2020.
- [2] D. Beymer and D. M. Russell, "Webgazeanalyser: a system for capturing and analyzing web reading behavior using eye gaze," in *CHI'05 extended abstracts on Human factors in computing systems*, 2005, pp. 1913–1916.
- [3] N. Ramkumar, V. Kothari, C. Mills, R. Koppel, J. Blythe, S. Smith, and A. L. Kun, "Eyes on urls: Relating visual behavior to safety decisions," in *ACM Symposium on Eye Tracking Research and Applications*, 2020, pp. 1–10.
- [4] R. Dhamija, J. D. Tygar, and M. Hearst, "Why phishing works," in *Proc. of the SIGCHI conference on Human Factors in computing systems*, 2006, pp. 581–590.
- [5] I. Baxter. (2020) Fake login attack evades logo detection. <https://ironscales.com/blog/fake-login-attack-evades-logo-detection>.
- [6] Z. A. Wen, Z. Lin, R. Chen, and E. Andersen, "What. hack: engaging anti-phishing training through a role-playing phishing simulation game," in *Proceedings of the 2019 CHI Conference on Human Factors in Computing Systems*, 2019, pp. 1–12.
- [7] R. C. Dodge Jr, C. Carver, and A. J. Ferguson, "Phishing for user security awareness," *computers & security*, vol. 26, no. 1, pp. 73–80, 2007.
- [8] A. K. Jain and B. B. Gupta, "Phishing detection: analysis of visual similarity based approaches," *Security and Communication Networks*, vol. 2017, 2017.
- [9] M. Khonji, Y. Iraqi, and A. Jones, "Phishing detection: a literature survey," *IEEE Communications Surveys & Tutorials*, vol. 15, no. 4, pp. 2091–2121, 2013.
- [10] S. Egelman, L. F. Cranor, and J. Hong, "You've been warned: an empirical study of the effectiveness of web browser phishing warnings," in *Proceedings of the SIGCHI Conference on Human Factors in Computing Systems*, 2008, pp. 1065–1074.
- [11] E. Al-Shaer, J. Wei, W. Kevin, and C. Wang, "Autonomous cyber deception," *Springer*, 2019.
- [12] L. Huang and Q. Zhu, "A dynamic games approach to proactive defense strategies against advanced persistent threats in cyber-physical systems," *Computers & Security*, vol. 89, p. 101660, 2020.
- [13] J. Pawlick and Q. Zhu, *Game Theory for Cyber Deception: From Theory to Applications*. Springer Nature, 2021.
- [14] C. Katsini, Y. Abdrabou, G. E. Raptis, M. Khamis, and F. Alt, "The role of eye gaze in security and privacy applications: survey and future hci research directions," in *Proceedings of the 2020 CHI Conference on Human Factors in Computing Systems*, 2020, pp. 1–21.

- [15] D. Miyamoto, G. Blanc, and Y. Kadobayashi, “Eye can tell: On the correlation between eye movement and phishing identification,” in *Int. Conf. on Neural Information Processing*. Springer, 2015, pp. 223–232.
- [16] E. B. Cox, Q. Zhu, and E. Balceris, “Stuck on a phishing lure: differential use of base rates in self and social judgments of susceptibility to cyber risk,” *Comprehensive Results in Social Psychology*, vol. 4, no. 1, pp. 25–52, 2020.
- [17] J. McAlaney and P. J. Hills, “Understanding phishing email processing and perceived trustworthiness through eye tracking,” *Front. Psychol.*, vol. 11, p. 1756, 2020.
- [18] A. Xiong, R. W. Proctor, W. Yang, and N. Li, “Is domain highlighting actually helpful in identifying phishing web pages?” *Hum. Factors*, vol. 59, no. 4, pp. 640–660, 2017.
- [19] K. Pfeffel, P. Ulsamer, and N. H. Müller, “Where the user does look when reading phishing mails—an eye-tracking study,” in *Int. Conf. on Human-Computer Interaction*. Springer, 2019, pp. 277–287.
- [20] D. J. Liebling and S. Preibusch, “Privacy considerations for a pervasive eye tracking world,” in *Proceedings of the 2014 ACM International Joint Conference on Pervasive and Ubiquitous Computing: Adjunct Publication*, 2014, pp. 1169–1177.
- [21] J. L. Kröger, O. H.-M. Lutz, and F. Müller, “What does your gaze reveal about you? on the privacy implications of eye tracking,” in *IFIP International Summer School on Privacy and Identity Management*. Springer, 2019, pp. 226–241.
- [22] R. M. Yerkes, J. D. Dodson *et al.*, “The relation of strength of stimulus to rapidity of habit-formation,” *Punishment: Issues and experiments*, pp. 27–41, 1908.
- [23] P. I. Frazier, “Bayesian optimization,” in *Recent Advances in Optimization and Modeling of Contemporary Problems*. INFORMS, 2018, pp. 255–278.